ACS APPLIED MATERIALS & INTERFACES

Research Article

www.acsami.org

Label-Free Luminescent Switch-On Probe for Ochratoxin A Detection Using a G-Quadruplex-Selective Iridium(III) Complex

Lihua Lu,[†] Modi Wang,[†] Li-Juan Liu,[‡] Chung-Hang Leung,*[,‡] and Dik-Lung Ma*[,†,§]

[†]Department of Chemistry, Hong Kong Baptist University, Kowloon Tong, Hong Kong, China

[‡]State Key Laboratory of Quality Research in Chinese Medicine, Institute of Chinese Medical Sciences, University of Macau, Macao, China

[§]Partner State Key Laboratory of Environmental and Biological Analysis, Hong Kong Baptist University, Hong Kong, China

Supporting Information

ABSTRACT: A library of six luminescent Ir(III) complexes were synthesized and studied for their capacity to function as probes for G-quadruplex DNA. The novel Ir(III) complex **1** was discovered to be selective for G-quadruplex structures and was subsequently used for the construction of a label-free G-quadruplex-based ochratoxin A (OTA) sensing platform in aqueous solution. The assay exhibited linearity for OTA in the range of 0 to 60 nM (R^2 = 0.9933), and the limit of detection for OTA was 5 nM. Furthermore, this assay was highly selective for OTA over its structurally related analogues.

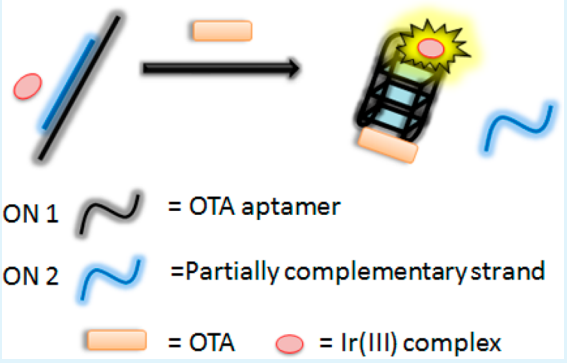

KEYWORDS: *G-quadruplex, iridium(III) complex, label-free, ochratoxin A, luminescent*

INTRODUCTION

Ochratoxin A (OTA) is a secondary metabolite manufactured by fungal species such as *Aspergillus ochraceus* and *Penicillium verrucosum* and is widely present in soil, animals, plants, and various foodstuffs.[1−4] Extensive studies have shown that OTA causes nephrotoxic, carcinogenic, hepatotoxic, teratogenic, and immunotoxic effects to humans.[5−9] Thusly, OTA has been categorized as a potential carcinogen (group 2B), and countries have established limits to OTA levels in food and beverages.[10,11]

The discovery of simple and facile OTA detection assays to prevent the consumption of OTA by humans is therefore highly required. Chromatographic techniques including gas chromatography (GC),[12] high-performance liquid chromatography (HPLC),[13−16] and liquid chromatography-tandem mass spectrometry (LC-MS)[17−19] have been employed to detect OTA contamination. However, these techniques tend to require expensive instrumentation, long processing times, and specially trained personnel. The enzyme-linked immunosorbent assay (ELISA) is relatively simpler but still necessitates the use of protein antibodies that can be unstable and/or tedious to prepare.[20−25] In contrast, nucleic acid aptamers are generally more robust under various conditions, and their binding abilities can be retained even after many times of denaturation−renaturation cycles.[8] In 2008, Cruz-Aguado and Penner reported the 36-nt OTA aptamer that binds to OTA, with a K_d value of 200 nM.[26,27] Interestingly, the binding is accompanied by a transition of the aptamer from a random single-stranded DNA (ssDNA) conformation into an antiparallel G-quadruplex structure. The "structure-switching" response of the OTA aptamer has been transduced into luminescent,[28−36] colorimetric,[37−41] or electrochemical signals[42−45] in various OTA detection assays. However, the majority of aptamer-based assays for OTA detection have required labeled oligonucleotides and/or multiple DNA probes.[46]

The G-quadruplex structure is a well-known nucleic acid secondary structure formed by planar arrays of guanine tetrads stabilized by Hoogsteen hydrogen bonding as well as metal cations.[47−50] The extensive structural diversity of G-quadruplexes has made them as versatile signal transducers for the construction of label-free detection platforms for environmentally or biologically important analytes.[51−53] In the label-free approach, it is crucial for the G-quadruplex-selective ligand to exhibit a high affinity and specificity for G-quadruplex DNA. However, some commonly used organic dyes, such as crystal violet, thiazole orange, and thioflavin T, show unrestricted binding to various DNA conformations.[54] At the same time, luminescent metal complexes have attracted great interest as probes for biomolecules due to their long lifetime, large Stokes shift, simple synthetic protocols, and adjustable excitation and emission maxima in the visible range.[54,55] We have previously

Received: February 24, 2015
Accepted: April 3, 2015
Published: April 3, 2015

DOI: 10.1021/acsami.5b01702
ACS Appl. Mater. Interfaces 2015, 7, 8313−8318

discovered that octahedral Ir(III) complexes can be harnessed to develop probes that are selective for G-quadruplex DNA.[56−59] Therefore, we aimed to construct a label-free luminescent switch-on sensing assay for OTA using Ir(III) complexes and the OTA aptamer.

EXPERIMENTAL SECTION

Materials. OTA, OTB, and warfarin were purchased from Sigma-Aldrich (St. Louis, MO) and used as received. Iridium chloride hydrate ($IrCl_3 \cdot xH_2O$) was purchased from Precious Metals Online (Australia). Other reagents, unless specified, were also purchased from Sigma-Aldrich (St. Louis, MO). All oligonucleotides were purchased from Techdragon Inc. (Hong Kong, China).

G4-FID Assay. The assay was performed as previously described.[60]

Absorption Titration. The titration was performed as previously described.[61]

Detection of OTA in Buffered Solution. The random-coil OTA aptamers ON1 (100 μM) and ON2 (100 μM) were annealed in Tris-HCl buffer (20 mM, pH 7.0). The annealed DNA was placed at −20 °C before use. For assaying OTA, 500 μL of OTA binding buffer (10 mM Tris-HCl, 120 mM NaCl, 10 mM $MgCl_2$, 10 mM KCl, pH 8.4) with the indicated concentrations of OTA was added to the solution containing the double-stranded DNA (0.5 μM). The mixture was placed at 25 °C for 10 min to allow the formation of the G-quadruplex to take place. Finally, 0.5 μM of complex **1** was added to the mixture. Emission spectra were recorded in the 550−750 nm range while λ_{ex} = 310 nm.

RESULTS AND DISCUSSION

Ir(III) complexes **1**−**6** (Figure 1) carrying the C^N ligand 1-phenylisoquinoline (piq) and N^N ligands based on 1,10-

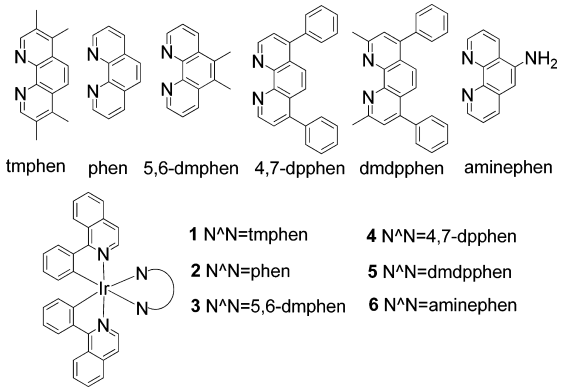

Figure 1. Molecular structures of Ir(III) complexes **1**−**6** used in this study.

phenatheroline (phen) were used in the present study (Table S1, Supporting Information). These complexes emit at λ > 590 nm; therefore, interference from the fluorescence of OTA (λ_{em} = 435 nm) should be minimal. Complexes **1**−**6** were initially tested for their capacity to discriminate G-quadruplex (G4) from double-stranded DNA (dsDNA) and ssDNA (Table S2, Supporting Information). Interestingly, the novel complex **1** $[Ir(piq)_2(tmphen)]^+$ (where tmphen = 3,4,7,8-tetramethyl-1,10-phenanthroline) showed an excellent discrimination for G-quadruplex DNA, with the highest I_{G4}/I_{dsDNA} and I_{G4}/I_{ssDNA} values among the six complexes tested (Figure 2). Complex **1** also exhibited the strongest luminescence response to the PS2.M G-quadruplex (ca. 5.9-fold), while only slight luminescence changes were observed for ssDNA (CCR5-DEL) and dsDNA (ds17) (Figure S1a,g, Supporting Information). On the other hand, complexes **2**−**6** showed

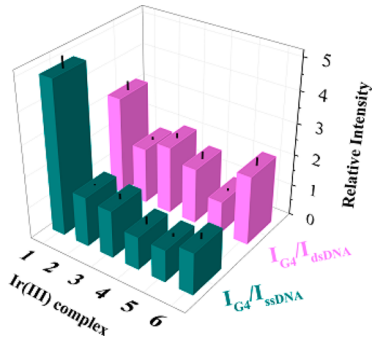

Figure 2. Bar array chart showing the luminescence enhancement selectivity ratio of complexes **1**−**6** for G-quadruplex DNA (PS2.M) over dsDNA (ds17) and ssDNA (CCR5-DEL). Error bars show the standard deviations of the results from three independent experiments.

little or no selectivity for G-quadruplex DNA (Figure S1b−g, Supporting Information). Of the six iridium(III) complexes tested, complexes **4** and **5** containing two substituted benzene rings showed the lowest enhancement to G-quadruplex DNA, which could be attributed to their relatively bulky molecular structure. Complex **1** possessing four methyl groups at the 3, 4, 7, and 8 positions of the 1,10-phenanthroline N^N ligand exhibited the highest emission increase to the G-quadruplex structure. Complex **2**, which has no substituents, and complexes **3** and **6**, which have two methyl groups and an amine group, respectively, on the 1,10-phenanthroline core showed lower luminescent enhancements to G-quadruplex DNA. These results suggest that the specificity of the complexes for G-quadruplex DNA are dependent on their molecular structure, including molecular size and substitution pattern.

The specific binding of complex **1** toward G-quadruplex structures was also confirmed by FRET-melting assay, UV/vis absorption titration experiment, and G-quadruplex fluorescent intercalator displacement (G4-FID) experiments. The melting temperature (ΔT_m) of the F21T G-quadruplex was raised by approximately 16 °C in the presence of **1** (Figure 3a). On the other hand, **1** increased the melting temperature of F10T dsDNA by only 6 °C under the same conditions (Figure 3b). Additionally, the UV/vis absorption titration assay showed that the binding constant of **1** for the PS2.M G-quadruplex is 1.26 × 10^5 M^{-1} (Figure S2a, Supporting Information), which is about 3-fold and 6-fold higher than that for dsDNA (0.4 × 10^5 M^{-1}, Figure S2b, Supporting Information) or ssDNA (0.21 × 10^5 M^{-1}, Figure S2c, Supporting Information), respectively. The G4-FID assay revealed that **1** could displace thiazole orange (TO) from G-quadruplex DNA with a $^{G4}DC_{50}$ value (half-maximal concentration of compound required to displace 50% TO from DNA) of 4.2 μM (Figure 3c). By comparison, even at the highest concentrations of **1** tested, less than 50% of TO was displaced from dsDNA. In summary, these data show that complex **1** interacts selectively with G-quadruplex DNA over either dsDNA or ssDNA. As far as we are aware, the G-quadruplex-binding selectivity of **1** has not been previously reported. To additionally study the role of the loop regions of the G-quadruplex structure in the interaction between complex **1** and G-quadruplex DNA, we examined the emission response of **1** to different G-quadruplex DNA structures, including structures containing a 5′-side loop (5′-$G_3T_nG_3T_3G_3T_3G_3$-3′), a central loop (5′-$G_3T_3G_3T_nG_3T_3G_3$-3′), or a 3′-side loop (5′-$G_3T_3G_3T_3G_3T_nG_3$-3′), with loop lengths ranging from 1 to 15 nucleotides (nt) (Figure 3d−f). The results revealed that the

DOI: 10.1021/acsami.5b01702
ACS Appl. Mater. Interfaces 2015, 7, 8313−8318

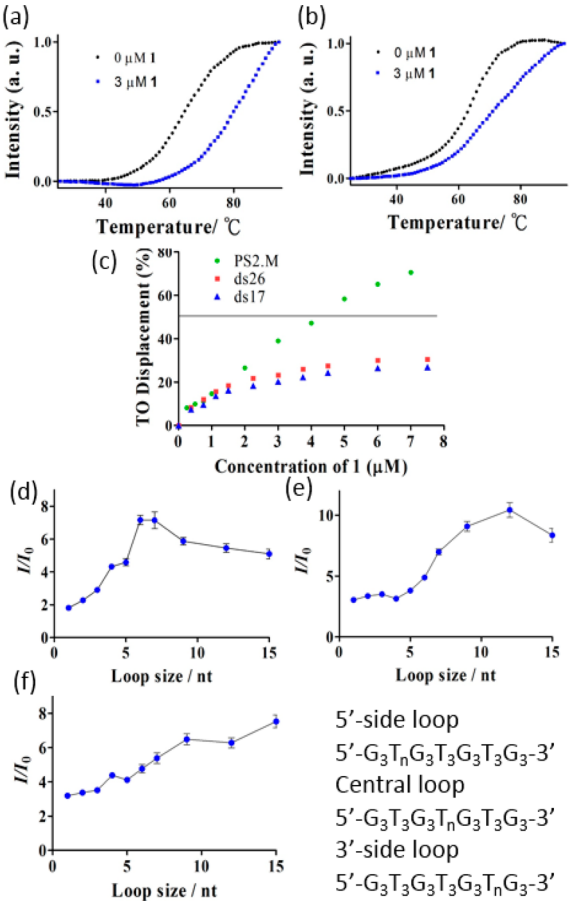

Figure 3. (a) Melting profile of F21T G-quadruplex DNA (0.2 μM) with and without **1** (3 μM). (b) Melting profile of F10T dsDNA (0.2 μM) with and without **1** (3 μM). (c) G4-FID titration curves of DNA duplex ds17 and ds26 and G-quadruplex DNA PS2.M in the presence of increasing concentration of complex **1** in Tris-HCl buffer. ($^{G4}DC_{50}$ value is defined by the half-maximal concentration of compound required to displace 50% TO from G-quadruplex DNA). Emission enhancement of **1** at different loop sizes: (d) 5′-side loop, (e) central loop, and (f) 3′-side loop (in nucleotides).

emission of complex **1** was positively correlated with loop size, for all kinds of loops. As the loop size was lengthened from 1 to 15 nt, the emission of complex **1** was enhanced from 1.8- to 7.1-fold (5′-side loop), from 3.1- to 10.5-fold (central loop), and from 3.2- to 7.5-fold (3′-side loop). This data indicates that the loop region of the G-quadruplex structure may be a significant determinant in the binding interaction between complex **1** and the G-quadruplex motif. This finding is also consistent with prior studies reported by Qu and co-workers,[62] who reported the binding between ligands and G-quadruplex structures could depend on the nature of the loop region.

The proposed mechanism of the aptamer-based sensing assay for OTA using the luminescent G-quadruplex-selective Ir(III) probe is depicted in Scheme 1. The oligonucleotide sequence ON1 containing the OTA aptamer (5′-GATCG$_3$TGTG$_3$T-G$_2$CGTA$_3$G$_3$AGCATCG$_2$ACA-3′) is initially located within a duplex substrate via hybridization with a partially complementary DNA strand ON2 (5′-C$_2$ACAC$_3$GATC-3′). The addition of OTA can cause ON1 to dissociate from ON2 due to the strong affinity of the OTA aptamer for OTA, allowing ON1 to fold into a quadruplex structure. The OTA G-quadruplex aptamer is then bound by the G-quadruplex-

Scheme 1. Schematic Representation of the Label Free OTA Assay Based on a Duplex Substrate and G-Quadruplex Selective Luminescent Probe

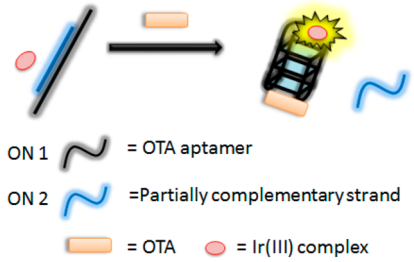

selective Ir(III) complex **1** with an increased emission response, enabling this system to act as a switch-on label-free luminescent detection platform for OTA. Moreover, this duplex-to-quadruplex approach is advantageous compared to a random coil-to-quadruplex strategy because the initial duplex substrate may be more resistant to the presence of interfering ions, such as K^+ and Na^+, which may induce single-stranded OTA aptamer into a G-quadruplex motif even without the addition of OTA.

We first studied the emission response of **1** and the ON1/ON2 duplex to OTA in buffered solution. It was seen that the emission of **1** was significantly increased when OTA was added. To confirm that the observed emission increase arose from the generation of the OTA-induced G-quadruplex, we performed several control experiments. No notable enhancement in emission was seen when OTA was added to **1** in the absence of ON1/ON2, indicating that **1** did not interact with OTA directly (Figure S3, Supporting Information). We also tested a duplex substrate (ON1$_m$, 5′-GATCT_3TGTC_3TG$_2$CGT-A$_3$C$_3$AGCATCG$_2$ACA-3′; ON2$_m$, 5′-G$_2$ACAA$_3$GATC-3′) that cannot fold into a G-quadruplex structure in response to OTA due to the absence of critical guanine bases. As anticipated, only a small emission increase was detected at 60 nM OTA for the mutant duplex, suggesting that the generation of the G-quadruplex structure is critical for the mechanism of this assay (Figure S4, Supporting Information). Circular dichroism (CD) spectroscopy was also used to confirm the duplex-to-quadruplex conformational transition induced by OTA (Figure S5, Supporting Information). The CD spectrum of the ON1/ON2 duplex without OTA shows a positive peak at 270 nm and a pronounced negative peak at 240 nm, which is suggestive for duplex DNA. Upon the addition of OTA, a positive band at 290 nm and a weak negative peak at 250 nm are observed, consistent with previous reports on the OTA aptamer G-quadruplex.[63] In summary, this data indicates that the emission increase of the detection platform can be attributed to the specific binding of complex **1** with the OTA aptamer G-quadruplex.

After optimization of the concentrations of duplex DNA and complex **1** (Figures S6 and S7, Supporting Information), the emission response of the assay to a range of OTA concentrations (5 to 150 nM) was tested. The system showed a ca. 4.8-fold increase in luminescence at [OTA] = 150 nM (Figure 4a), with linearity for OTA from 0 to 60 nM (Figure 4b). We estimated the detection limit of this assay for OTA to be 5 nM at a signal-to-noise ratio (S/N) of 3 (Figure S8, Supporting Information). This detection limit is on the same order of magnitude as other aptamer-based luminescent methods reported in the literature.[28,35,64] Moreover, this

DOI: 10.1021/acsami.5b01702
ACS Appl. Mater. Interfaces 2015, 7, 8313−8318

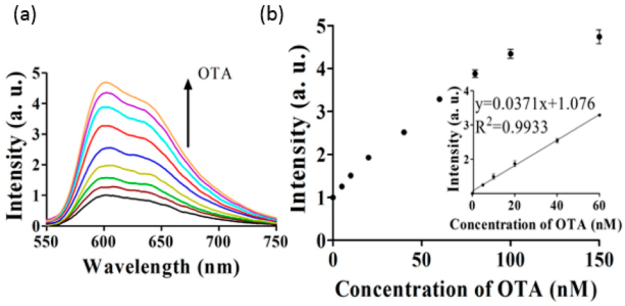

Figure 4. (a) Emission spectra of the **1**/duplex DNA system with different concentrations of OTA: 5, 10, 20, 40, 60, 80, 100, and 150 nM. (b) The relationship between emission intensity at λ = 600 nm and OTA concentration. Inset: linear plot of the change in luminescence intensity at λ = 600 nm vs OTA concentration. Error bars show the standard deviations of the results from three independent experiments.

detection limit is similar to the safe upper limit of OTA (2 μg/L) contamination in beer, wine, and grape juice.[1,4]

The selectivity of this detection platform for OTA was examined by evaluating the luminescent response of the detection platform to structurally related analogues of OTA, such as ochratoxin B (OTB) and warfarin (WF). The data showed that only OTA could significantly increase the emission of the complex **1**/duplex DNA system (Figure 5), while no

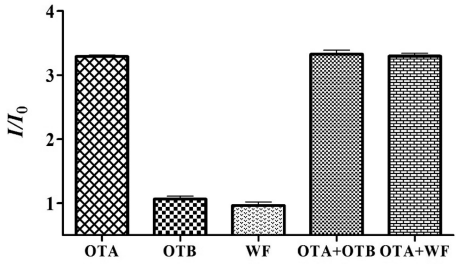

Figure 5. Selectivity of the G-quadruplex-based OTA detection over its analogues. The concentration of OTA was 60 nM, and the concentrations of the OTA analogues were 60 nM. Error bars show the standard deviations of the results from three independent experiments.

signal enhancement with the structural analogues of OTA was observed. This data indicates that the system displays notable selectivity for OTA over structurally related compounds, which is attributed to the specific interaction of the OTA aptamer for OTA.

CONCLUSION

In summary, the novel luminescent Ir(III) complex **1** was discovered to display excellent selectivity for G-quadruplex structures over other types of DNA, including dsDNA and ssDNA, and was utilized for the development of a G-quadruplex-based detection platform for OTA. When OTA is absent, the DNA substrate initially exists in a duplex structure that binds inefficiently with **1**. However, the addition of OTA significantly enhances the emission of the system due to the conformational shift of the DNA duplex into a G-quadruplex motif, that is recognized by complex **1**. Additionally, this probe showed robust selectivity for OTA over its structural analogues. This label-free G-quadruplex-based luminescence switch-on platform is simple, rapid, and cost-effective compared to conventional chromatographic or immunological assays.

ASSOCIATED CONTENT

Supporting Information

Experimental section; photophysical properties of iridium(III) complexes **1**–**6**; DNA sequences used in this project; luminescence response of complexes **1**–**6** in 20 mM Tris buffer; plot of $D/\Delta\varepsilon ap$ vs concentration of DNA for estimating the intrinsic binding constant (K); luminescence response of the system with the complex **1** alone in the absence and presence of OTA; relative luminescence response of complex **1** in the presence of OTA and duplex DNA or duplex DNA mutant; circular dichroism (CD) spectrum; relative luminescence response of the system in the absence or presence of OTA at various concentrations of duplex DNA; relative luminescence response of the system in the absence or presence of OTA at various concentrations of complex **1**; emission spectral traces of complex **1** and duplex DNA in the presence of OTA. This material is available free of charge via the Internet at http://pubs.acs.org.

AUTHOR INFORMATION

Corresponding Authors

*E-mail: edmondma@hkbu.edu.hk (D.-L.M.).
*E-mail: duncanleung@umac.mo (C.-H.L.).

Notes

The authors declare no competing financial interest.

ACKNOWLEDGMENTS

This work is supported by Hong Kong Baptist University (FRG2/13-14/008 and FRG2/14-15/004), Centre for Cancer and Inflammation Research, School of Chinese Medicine (CCIR-SCM, HKBU), the Health and Medical Research Fund (HMRF/13121482 and HMRF/14130522), the Research Grants Council (HKBU/201811, HKBU/204612, and HKBU/201913), the French National Research Agency/Research Grants Council Joint Research Scheme (A-HKBU201/12), State Key Laboratory of Environmental and Biological Analysis Research Grant (SKLP-14-15-P001), the State Key Laboratory of Synthetic Chemistry, the Science and Technology Development Fund, Macao SAR (103/2012/A3), and the University of Macau (MYRG091(Y3-L2)-ICMS12-LCH, MYRG2015-00137-ICMS-QRCM, and MRG023/LCH/2013/ICMS).

REFERENCES

(1) Ali, W. H.; Pichon, V. Characterization of Oligosorbents and Application to the Purification of Ochratoxin A from Wheat Extracts. *Anal. Bioanal. Chem.* **2014**, *406*, 1233–1240.
(2) Elmholt, S.; Hestbjerg, H. Field Ecology of The Ochratoxin A-Producing Penicillium Verrucosum: Survival and Resource Colonisation in Soil. *Mycopathologia* **1999**, *147*, 67–81.
(3) Casal, S.; Vieira, T.; Cruz, R.; Cunha, S. C. Ochratoxin A in Commercial Soluble Coffee and Coffee Substitutes. *Food Res. Int.* **2014**, *61*, 56–60.
(4) Copetti, M. V.; Iamanaka, B. T.; Pitt, J. I.; Taniwaki, M. H. Fungi and Mycotoxins in Cocoa: From Farm to Chocolate. *Int. J. Food Microbiol.* **2014**, *178*, 13–20.
(5) Domijan, A. M.; Gajski, G.; Jovanovic, I. N.; Genic, M.; Garaj-Vrhovac, V. In Vitro Genotoxicity of Mycotoxins Ochratoxin A and Fumonisin B-1 Could be Prevented by Sodium Copper Chlorophyllin - Implication to Their Genotoxic Mechanism. *Food Chem.* **2015**, *170*, 455–462.

DOI: 10.1021/acsami.5b01702
ACS Appl. Mater. Interfaces 2015, 7, 8313–8318

(6) Vettorazzi, A.; Gonzalez-Penas, E.; de Cerain, A. L. Ochratoxin A Kinetics: A Review of Analytical Methods and Studies in Rat Model. *Food Chem. Toxicol.* **2014**, *72*, 273−288.
(7) Malir, F.; Ostry, V.; Pfohl-Leszkowicz, A.; Novotna, E.; Ochratoxin, A. Developmental and Reproductive Toxicity-An Overview. *Birth Defects Res., Part B* **2013**, *98*, 493−502.
(8) Sorrenti, V.; Di Giacomo, C.; Acquaviva, R.; Barbagallo, I.; Bognanno, M.; Galvano, F. Toxicity of Ochratoxin A and Its Modulation by Antioxidants: A Review. *Toxins* **2013**, *5*, 1742−1766.
(9) Pfohl-Leszkowicz, A.; Manderville, R. A. Ochratoxin A: An Overview on Toxicity and Carcinogenicity in Animals and Humans. *Mol. Nutr. Food Res.* **2007**, *51*, 61−99.
(10) IARC *Monographs online*; IARC: Lyon, 1993; Vol. *56*, pp 489−521.
(11) Marino-Repizo, L.; Kero, F.; Vandell, V.; Senior, A.; Isabel Sanz-Ferramola, M.; Cerutti, S.; Raba, J. A Novel Solid Phase Extraction - Ultra High Performance Liquid Chromatography-Tandem Mass Spectrometry Method for the Quantification of Ochratoxin A in Red Wines. *Food Chem.* **2015**, *172*, 663−668.
(12) Amelin, V. G.; Karaseva, N. M.; Tretyakov, A. V. Simultaneous Determination of Trichothecene Micotoxins, Ochratoxin A, and Zearalenone in Grain and Products of Its Processing, Feed Premixes, and Meat by Gas Chromatography. *J. Anal. Chem.* **2013**, *68*, 61−67.
(13) Andrade, P. D.; da Silva, J. L. G.; Caldas, E. D. Simultaneous Analysis of Aflatoxins BI, B2, G-1, G2, M-1 and Ochratoxin A in Breast Milk by High-Performance Liquid Chromatography/Fluorescence after Liquid-Liquid Extraction with Low Temperature Purification-(LLE-LTP). *J. Chromatogr. A* **2013**, *1304*, 61−68.
(14) Arroyo-Manzanares, N.; Garcia-Campana, A. M.; Gamiz-Gracia, L. Comparison of Different Sample Treatments for the Analysis of Ochratoxin A in Wine by Capillary HPLC with Laser-Induced Fluorescence Detection. *Anal. Bioanal. Chem.* **2011**, *401*, 2987−2994.
(15) Attya, M.; Di Donna, L.; Mazzotti, F.; Fazio, A.; Gabriele, B.; Sindona, G. Detection of Ochratoxin A Based on the Use of Its Diastereoisomer as an Internal Standard. *Anal. Methods* **2014**, *6*, 5610−5614.
(16) Giovannoli, C.; Passini, C.; Di Nardo, F.; Anfossi, L.; Baggiani, C. Determination of Ochratoxin A in Italian Red Wines by Molecularly Imprinted Solid Phase Extraction and HPLC Analysis. *J. Agric. Food Chem.* **2014**, *62*, 5220−5225.
(17) Campone, L.; Piccinelli, A. L.; Rastrelli, L. Dispersive Liquid-Liquid Microextraction Combined with High-Performance Liquid Chromatography-Tandem Mass Spectrometry for the Identification and the Accurate Quantification by Isotope Dilution Assay of Ochratoxin A in Wine Samples. *Anal. Bioanal. Chem.* **2011**, *399*, 1279−1286.
(18) Duarte, S. C.; Lino, C. M.; Pena, A. Novel IAC-LC-ESI-MS(2) Analytical Set-Up for Ochratoxin A Determination in Pork. *Food Chem.* **2013**, *138*, 1055−1061.
(19) Fernandes, P. J.; Barros, N.; Camara, J. S. A Survey of the Occurrence of Ochratoxin A in Madeira Wines Based on a Modified QuEChERS Extraction Procedure Combined with Liquid Chromatography-Triple Quadrupole Tandem Mass Spectrometry. *Food Res. Int.* **2013**, *54*, 293−301.
(20) Laura, A.; Gilda, D. A.; Claudio, B.; Cristina, G.; Gianfranco, G. A Lateral Flow Immunoassay for Measuring Ochratoxin A: Development of a Single System for Maize, Wheat and Durum Wheat. *Food Control* **2011**, *22*, 1965−1970.
(21) Lippolis, V.; Pascale, M.; Valenzano, S.; Porricelli, A. C. R.; Suman, M.; Visconti, A. Fluorescence Polarization Immunoassay for Rapid, Accurate and Sensitive Determination of Ochratoxin A in Wheat. *Food Anal. Methods* **2014**, *7*, 298−307.
(22) Meulenberg, E. P. Immunochemical Methods for Ochratoxin A Detection: A Review. *Toxins* **2012**, *4*, 244−266.
(23) Moon, J.; Kim, G.; Lee, S. Development of Nanogold-Based Lateral Flow Immunoassay for the Detection of Ochratoxin A in Buffer Systems. *J. Nanosci. Nanotechnol.* **2013**, *13*, 7245−7249.
(24) Novo, P.; Moulas, G.; Prazeres, D. M. F.; Chu, V.; Conde, J. P. Detection of Ochratoxin A in Wine and Beer by Chemiluminescence-Based ELISA in Microfluidics with Integrated Photodiodes. *Sens. Actuators, B* **2013**, *176*, 232−240.
(25) Yu, F. Y.; Vdovenko, M. M.; Wang, J. J.; Sakharov, I. Y. Comparison of Enzyme-Linked Immunosorbent Assays with Chemiluminescent and Colorimetric Detection for the Determination of Ochratoxin A in Food. *J. Agric. Food Chem.* **2011**, *59*, 809−813.
(26) Jorge, A. C.-A.; Gregory, P. Determination of Ochratoxin A with a DNA Aptamer. *J. Agric. Food Chem.* **2008**, *56*, 6.
(27) Rhouati, A.; Yang, C.; Hayat, A.; Marty, J.-L. Aptamers: A Promising Tool for Ochratoxin A Detection in Food Analysis. *Toxins* **2013**, *5*, 1988−2008.
(28) Zhao, Q.; Geng, X.; Wang, H. Fluorescent Sensing Ochratoxin A with Single Fluorophore-Labeled Aptamer. *Anal. Bioanal. Chem.* **2013**, *405*, 6281−6286.
(29) Zhao, Q.; Lv, Q.; Wang, H. L. Identification of Allosteric Nucleotide Sites of Tetramethylrhodamine-Labeled Aptamer for Noncompetitive Aptamer-Based Fluorescence Anisotropy Detection of a Small Molecule, Ochratoxin A. *Anal. Chem.* **2014**, *86*, 1238−1245.
(30) Zhang, J.; Zhang, X.; Yang, G. D.; Chen, J. H.; Wang, S. H. A Signal-On Fluorescent Aptasensor Based on Tb^{3+} and Structure-Switching Aptamer for Label-Free Detection of Ochratoxin A in Wheat. *Biosens. Bioelectron.* **2013**, *41*, 704−709.
(31) Sheng, L.; Ren, J.; Miao, Y.; Wang, J.; Wang, E. PVP-Coated Graphene Oxide for Selective Determination of Ochratoxin A via Quenching Fluorescence of Free Aptamer. *Biosens. Bioelectron.* **2011**, *26*, 3494−3499.
(32) McKeague, M.; Velu, R.; Hill, K.; Bardoczy, V.; Meszaros, T.; DeRosa, M. C. Selection and Characterization of a Novel DNA Aptamer for Label-Free Fluorescence Biosensing of Ochratoxin A. *Toxins* **2014**, *6*, 2435−2452.
(33) Ma, W.; Yin, H. H.; Xu, L. G.; Xu, Z.; Kuang, H.; Wang, L. B.; Xu, C. L. Femtogram Ultrasensitive Aptasensor for the Detection of Ochratoxin A. *Biosens. Bioelectron.* **2013**, *42*, 545−549.
(34) Lv, Z.; Chen, A.; Liu, J.; Guan, Z.; Zhou, Y.; Xu, S.; Yang, S.; Li, C. A Simple and Sensitive Approach for Ochratoxin A Detection Using a Label-Free Fluorescent Aptasensor. *PloS One* **2014**, *9*, No. e85968.
(35) Chen, J.; Fang, Z.; Liu, J.; Zeng, L. A Simple and Rapid Biosensor for Ochratoxin A Based on a Structure-Switching Signaling Aptamer. *Food Control* **2012**, *25*, 555−560.
(36) Wang, L.; Chen, W.; Ma, W.; Liu, L.; Ma, W.; Zhao, Y.; Zhu, Y.; Xu, L.; Kuang, H.; Xu, C. Fluorescent Strip Sensor for Rapid Determination of Toxins. *Chem. Commun.* **2011**, *47*, 1574−1576.
(37) Yang, C.; Wang, Y.; Marty, J. L.; Yang, X. Aptamer-Based Colorimetric Biosensing of Ochratoxin A Using Unmodified Gold Nanoparticles Indicator. *Biosens. Bioelectron.* **2011**, *26*, 2724−2727.
(38) Yang, C.; Lates, V.; Prieto-Simon, B.; Marty, J. L.; Yang, X. Aptamer-DNAzyme Hairpins for Biosensing of Ochratoxin A. *Biosens. Bioelectron.* **2012**, *32*, 208−212.
(39) Wang, C.; Dong, X.; Liu, Q.; Wang, K. Label-Free Colorimetric Aptasensor for Sensitive Detection of Ochratoxin A Utilizing Hybridization Chain Reaction. *Anal. Chim. Acta* **2015**, *860*, 83−88.
(40) Lee, J.; Jeon, C. H.; Ahn, S. J.; Ha, T. H. Highly Stable Colorimetric Aptamer Sensors for Detection of Ochratoxin A through Optimizing the Sequence with the Covalent Conjugation of Hemin. *Analyst* **2014**, *139*, 1622−1627.
(41) Wang, L.; Ma, W.; Chen, W.; Liu, L.; Ma, W.; Zhu, Y.; Xu, L.; Kuang, H.; Xu, C. An Aptamer-Based Chromatographic Strip Assay for Sensitive Toxin Semi-Quantitative Detection. *Biosens. Bioelectron.* **2011**, *26*, 3059−3062.
(42) Tong, P.; Zhang, L.; Xu, J. J.; Chen, H. Y. Simply Amplified Electrochemical Aptasensor of Ochratoxin A Based on Exonuclease-Catalyzed Target Recycling. *Biosens. Bioelectron.* **2011**, *29*, 97−101.
(43) Rhouati, A.; Hayat, A.; Hernandez, D. B.; Meraihi, Z.; Munoz, R.; Marty, J. L. Development of an Automated Flow-Based Electrochemical Aptasensor for Online Detection of Ochratoxin A. *Sens. Actuators, B* **2013**, *176*, 1160−1166.
(44) Kuang, H.; Chen, W.; Xu, D.; Xu, L.; Zhu, Y.; Liu, L.; Chu, H.; Peng, C.; Xu, C.; Zhu, S. Fabricated Aptamer-Based Electrochemical

DOI: 10.1021/acsami.5b01702
ACS Appl. Mater. Interfaces 2015, 7, 8313−8318

"Signal-Off" Sensor of Ochratoxin A. *Biosens. Bioelectron.* **2010**, *26*, 710−716.
(45) Chen, Y.; Yang, M. L.; Xiang, Y.; Yuan, R.; Chai, Y. Q. Binding-Induced Autonomous Disassembly of Aptamer-DNAzyme Supersandwich Nanostructures for Sensitive Electrochemiluminescence Turn-On Detection of Ochratoxin A. *Nanoscale* **2014**, *6*, 1099−1104.
(46) Kaushik, A. Recent Advances in Detection of Ochratoxin-A. *Open J. Appl. Biosens.* **2013**, *02*, 1−11.
(47) Guédin, A.; Alberti, P.; Mergny, J.-L. Stability of Intramolecular Quadruplexes: Sequence Effects in the Central Loop. *Nucleic Acids Res.* **2009**, *37*, 5559−5567.
(48) Balasubramanian, S.; Hurley, L. H.; Neidle, S. Targeting G-Quadruplexes in Gene Promoters: A Novel Anticancer Strategy? *Nat. Rev. Drug Discovery* **2011**, *10*, 261−275.
(49) Guédin, A.; Gros, J.; Alberti, P.; Mergny, J.-L. How Long Is too Long? Effects of Loop Size on G-Quadruplex Stability. *Nucleic Acids Res.* **2010**, *38*, 7858−7868.
(50) Collie, G. W.; Parkinson, G. N. The Application of DNA and RNA G-Quadruplexes to Therapeutic Medicines. *Chem. Soc. Rev.* **2011**, *40*, 5867−5892.
(51) Tong, L.-l.; Li, L.; Chen, Z.; Wang, Q.; Tang, B. Stable Label-Free Fluorescent Sensing of Biothiols Based on ThT Direct Inducing Conformation-Specific G-Quadruplex. *Biosens. Bioelectron.* **2013**, *49*, 420−425.
(52) Li, T.; Dong, S.; Wang, E. Label-Free Colorimetric Detection of Aqueous Mercury Ion(Hg^{2+}) Using Hg^{2+}-Modulated G-Quadruplex-Based DNAzymes. *Anal. Chem.* **2009**, *81*, 2144−2149.
(53) Neo, J. L.; Kamaladasan, K.; Uttamchandani, M. G-Quadruplex Based Probes for Visual Detection and Sensing. *Curr. Pharm. Des.* **2012**, *18*, 2048−2057.
(54) Bhasikuttan, A. C.; Mohanty, J. Targeting G-Quadruplex Structures with Extrinsic Fluorogenic Dyes: Promising Fluorescence Sensors. *Chem. Commun.* **2015**, DOI: 10.1039/C4CC10030A.
(55) Yam, V. W.-W.; Wong, K. M.-C. Luminescent Metal Complexes of d^6, d^8 and d^{10} Transition Metal Centres. *Chem. Commun.* **2011**, *47*, 11579−11592.
(56) Ma, D.-L.; He, H.-Z.; Leung, K.-H.; Zhong, H.-J.; Chan, D. S.-H.; Leung, C.-H. Label-Free Luminescent Oligonucleotide-Based Probes. *Chem. Soc. Rev.* **2013**, *42*, 3427−3440.
(57) Monchaud, D.; Allain, C.; Bertrand, H.; Smargiasso, N.; Rosu, F.; Gabelica, V.; De Cian, A.; Mergny, J. L.; Teulade-Fichou, M. P. Ligands Playing Musical Chairs with G-Quadruplex DNA: A Rapid and Simple Displacement Assay for Identifying Selective G-Quadruplex Binders. *Biochimie* **2008**, *90*, 1207−1223.
(58) He, H.-Z.; Leung, K.-H.; Yang, H.; Chan, D. H.-S.; Leung, C.-H.; Zhou, J.; Bourdoncle, A.; Mergny, J.-L.; Ma, D.-L. Label-Free Detection of Sub-Nanomolar Lead(II) Ions in Aqueous Solution Using A Metal-Based Luminescent Switch-on Probe. *Biosens. Bioelectron.* **2013**, *41*, 871−874.
(59) He, H.-Z.; Leung, K.-H.; Wang, W.; Chan, D. S.-H.; Leung, C.-H.; Ma, D.-L. Label-Free Luminescence Switch-on Detection of T4 Polynucleotide Kinase Activity Using a G-Quadruplex-Selective Probe. *Chem. Commun.* **2014**, *50*, 5313−5315.
(60) Leung, K.-H.; He, H.-Z.; Wang, W.; Zhong, H.-J.; Chan, D. S.-H.; Leung, C.-H.; Ma, D.-L. Label-Free Luminescent Switch-on Detection of Endonuclease IV Activity Using a G-Quadruplex-Selective Iridium(III) Complex. *ACS Appl. Mater. Inter.* **2013**, *5*, 12249−12253.
(61) Kumar, C. V.; Asuncion, E. H. DNA Binding Studies and Site Selective Fluorescence Sensitization of an Anthryl Probe. *J. Am. Chem. Soc.* **1993**, *115*, 8547−8553.
(62) Yu, H.; Zhao, C.; Chen, Y.; Fu, M.; Ren, J.; Qu, X. DNA Loop Sequence as the Determinant for Chiral Supramolecular Compound G-Quadruplex Selectivity. *J. Med. Chem.* **2010**, *53*, 492−498.
(63) Chen, J.; Zhang, X.; Cai, S.; Wu, D.; Chen, M.; Wang, S.; Zhang, J. A Fluorescent Aptasensor Based on DNA-Scaffolded Silver-Nanocluster for Ochratoxin A Detection. *Biosens. Bioelectron.* **2014**, *57*, 226−231.
(64) Guo, Z.; Ren, J.; Wang, J.; Wang, E. Single-Walled Carbon Nanotubes Based Quenching of Free FAM-Aptamer for Selective Determination of Ochratoxin A. *Talanta* **2011**, *85*, 2517−2521.

DOI: 10.1021/acsami.5b01702
ACS Appl. Mater. Interfaces 2015, 7, 8313−8318